OPEN

Immunogenicity and reactogenicity of heterologous ChAdOx1 nCoV-19/mRNA vaccination

Tina Schmidt [1], Verena Klemis[1,4], David Schub [1,4], Janine Mihm [2], Franziska Hielscher[1], Stefanie Marx[1], Amina Abu-Omar[1], Laura Ziegler[1], Candida Guckelmus[1], Rebecca Urschel[1], Sophie Schneitler [3], Sören L. Becker [3], Barbara C. Gärtner [3], Urban Sester [2] and Martina Sester [1 ✉]

Heterologous priming with the ChAdOx1 nCoV-19 vector vaccine followed by boosting with a messenger RNA vaccine (BNT162b2 or mRNA-1273) is currently recommended in Germany, although data on immunogenicity and reactogenicity are not available. In this observational study we show that, in healthy adult individuals ($n = 96$), the heterologous vaccine regimen induced spike-specific IgG, neutralizing antibodies and spike-specific CD4 T cells, the levels of which which were significantly higher than after homologous vector vaccine boost ($n = 55$) and higher or comparable in magnitude to homologous mRNA vaccine regimens ($n = 62$). Moreover, spike-specific CD8 T cell levels after heterologous vaccination were significantly higher than after both homologous regimens. Spike-specific T cells were predominantly polyfunctional with largely overlapping cytokine-producing phenotypes in all three regimens. Recipients of both the homologous vector regimen and the heterologous vector/mRNA combination reported greater reactogenicity following the priming vector vaccination, whereas heterologous boosting was well tolerated and comparable to homologous mRNA boosting. Taken together, heterologous vector/mRNA boosting induces strong humoral and cellular immune responses with acceptable reactogenicity profiles.

Among the currently authorized COVID-19 vaccines, the ChAdOx1 nCoV-19 adenovirus-based vector vaccine (ChAdOx1) and the two mRNA vaccines (BNT162b2 and mRNA-1273) have been the most widely used. Both vaccine types are immunogenic and have shown remarkable efficacy in preventing COVID-19 disease[1–3]. In March 2021, administration of the ChAdOx1 vaccine was temporarily suspended in Germany due to the occurrence of life-threatening cerebral venous thrombosis and thrombocytopenia, primarily in younger women[4,5]. This resulted in revised recommendations for secondary vaccination of all individuals who had received the first dose of the vaccine[6]. Individuals above the age of 60 years are recommended to complete vaccination with the vector vaccine, whereas heterologous boosting with an mRNA vaccine is recommended in those <60 years, with the option to voluntarily remain on a homologous vector regimen[6]. Comparative analyses of immunogenicity between the authorized vaccine regimens

are scarce, and knowledge on immunity and reactogenicity after heterologous vaccination is currently limited. We have found that priming with the ChAdOx1 vaccine showed a stronger induction of spike-specific T cell responses as compared to mRNA priming, while antibody responses were more pronounced after mRNA priming[7]. We hypothesized that differences among the vaccine types after priming may influence cellular and humoral immunity following secondary vaccination. We therefore prospectively enrolled three groups of individuals to study the immunogenicity and reactogenicity of a heterologous vector/mRNA prime–booster regimen in comparison to the standard homologous regimens. A detailed analysis of spike-specific IgG levels and neutralizing antibody activity was performed. In addition, spike-specific CD4 and CD8 T cells were characterized using flow cytometry. Adverse events within the first week after the priming and booster doses were self-reported based on a standardized questionnaire.

A total of 216 immunocompetent individuals, primarily comprising employees, were prospectively enrolled at Saarland University Medical Center before secondary vaccination with the authorized vaccines ChAdOx1 nCoV-19, BNT162b2 or mRNA-1273 (Methods). Ninety-seven study participants received heterologous vaccination with the ChAdOx1 vector and mRNA booster (vector/mRNA), whereas 55 and 64 received homologous regimens with vector or mRNA vaccine, respectively (vector/vector and mRNA/mRNA; Extended Data Fig. 1). As per guidelines, the time between primary and secondary vaccination was shorter for mRNA-primed (4.3 ± 1.1 weeks) than for vector-primed individuals, with no difference between vector-based heterologous (11.2 ± 1.3 weeks) and homologous regimens (10.8 ± 1.4 weeks). Blood samples were drawn at a median of 14 (interquartile range (IQR) = 2) days after vaccination. Although all individuals had no known history of SARS-CoV-2 infection, three tested positive for SARS-CoV-2 nucleocapsid (N)-specific IgG and were excluded from further analyses. The groups had similar gender distribution. However, individuals on the homologous vector regimen were slightly older than the two other groups, who were of similar age (Extended Data Fig. 2). Leukocyte counts, including granulocytes, monocytes and lymphocytes, as well as major lymphocyte subpopulations such as CD4 and CD8 T cells, and B cells, did not differ between the groups. This also

held true for plasmablasts, which were identified as CD38-positive cells among IgD⁻CD27⁺ CD19-positive switched-memory B cells (Extended Data Fig. 2).

Spike-specific IgGs were induced in 212/213 individuals after vaccination. IgG levels after heterologous vaccination and homologous mRNA vaccination were similar (3,630 (IQR = 3721) and 4,932 (IQR = 4,239) BAU ml⁻¹, respectively), whereas levels after homologous vector vaccination were significantly lower (404 (IQR = 510) BAU ml⁻¹, $P < 0.0001$, two-sided Kruskal–Wallis test with Dunn´s multiple comparisons post test; Fig. 1a). This difference was also observed for neutralizing antibodies, which were quantified by a surrogate neutralization test. While the majority of individuals in the vector/mRNA and mRNA/mRNA groups had 100% inhibitory activity, this was significantly lower in the vector/vector group (Fig. 1b).

In the analysis of vaccine-induced T cell responses, overlapping peptide pools derived from the spike protein were used to stimulate whole-blood samples (Methods). Spike-specific CD4 and CD8 T cells were identified using flow cytometry by induction of CD69 and the cytokines interferon (IFN)-γ, tumor necrosis factor (TNF)-α and interleukin (IL)-2. The gating strategy and representative contour plots of cytokine-positive CD4 and CD8 T cells from a 37-year-old woman following heterologous vaccination are shown in Extended Data Fig. 3. Both the heterologous vector/mRNA and homologous mRNA/mRNA regimen led to a marked induction of spike-specific, IFN-γ-producing CD4 T cells with median percentages of 0.17 (IQR = 0.13%) and 0.16 (IQR = 0.19%), respectively, whereas CD4 T cell levels following homologous vector/vector vaccination were significantly lower (median 0.04% (IQR = 0.04%), each $P = 0.0001$; Fig. 1c). Interestingly, heterologous mRNA boosting in vector-primed individuals induced the highest percentages of spike-specific IFN-γ-producing CD8 T cells (0.28% (IQR = 0.54%)), which were not only more pronounced than after homologous vector boosting (vector/vector, 0.04% (IQR = 0.08%)) but also higher than for the mRNA/mRNA regimen (0.06% (IQR = 0.19))%, $P < 0.0001$; Fig. 1c). *Staphylococcus aureus* enterotoxin B (SEB)-reactive CD4 or CD8 T cell levels did not differ between groups (Fig. 1d). As with IFN-γ-producing CD4 and CD8 T cells, similar between-group differences were found for spike-specific CD4 T cells producing TNF-α or IL-2, and for spike-specific CD8 T cells producing TNF-α (Extended Data Fig. 4). Because CD8 T cells generally produce less IL-2, differences were less pronounced for IL-2-producing CD8 T cells. Finally, between-group differences were similar if CD4 or CD8 T cells producing any of the three cytokines were considered after Boolean gating (Extended Data Fig. 4).

An overview summarizing correlations between plasmablasts and spike-specific IgG and their neutralizing activity, and spike-specific CD4 and CD8 T cells, is shown in Fig. 1e and Supplementary Table 1. As expected, IgG levels showed a significant correlation with neutralizing activity in all three groups. A strong correlation was also found between spike-specific CD4 and CD8 T cell levels. In line with the role of CD4 T cells in supporting antibody production, CD4 T cells correlated with IgG levels in both the vector/vector and vector/mRNA groups. In the mRNA/mRNA group, antibody levels and neutralizing activity were found to correlate with CD8 T cell levels; whether this reflects a causal relationship or similar induction kinetics is currently unknown.

In addition to quantitative analysis of spike-specific CD4 and CD8 T cells, we also characterized the cytokine profiles of IFN-γ, IL-2 and TNF-α at the single-cell level. Based on the gating strategy shown in Extended Data Fig. 5, seven subpopulations—including multifunctional T cells producing all three cytokines—could be distinguished. When analyzed across all three participant groups, the majority of spike-specific CD4 T cells (42.5%) were multifunctional. In contrast, the dominant population among CD8 T cells consisted of dual-positive cells producing IFN-γ and TNF-α (47.3%), followed by 30.6% IFN-γ single-positive cells (Extended Data Fig. 5). The distribution of cytokine-producing cells showed significant differences between the three participant groups, which held true for both spike-specific CD4 and CD8 T cells (Fig. 1f). Given the particular ability of the vector vaccine to induce spike-specific T cells during priming[7], it is notable that the two vector-primed groups had the highest percentage of polyfunctional CD4 T cells irrespective of the boosting vaccine. This also held true for the dominant fraction of CD8 T cells coproducing IFN-γ and TNF-α. In contrast, SEB-reactive cytokine profiles among CD4 and CD8 T cells were similar in all vaccine groups (Extended Data Fig. 6).

Finally, local and systemic adverse events within the first week after primary and secondary vaccination were recorded using a questionnaire (Fig. 2a). Local reactions, such as pain at the injection site and swelling, were similar after priming with the vector and mRNA vaccines (Fig. 2b). However, participants reported significantly more systemic adverse events, including fever, chills, gastrointestinal events, headache, fatigue, myalgia or arthralgia, after the vector vaccine; participants also reported more frequent use of antipyretic drugs (Fig. 2c). When comparing reactogenicity after secondary vaccination, both local and systemic events were markedly less frequent in vector-primed individuals after the second vector booster. Boosting with an mRNA vaccine was less well tolerated in both vector- and mRNA-primed individuals, and the spectrum of local and systemic adverse events was very similar for both groups. Individual perception after the first or the second dose appears to be determined by the severity of the priming vector vaccine, as recipients of both the homologous vector and the heterologous vector/mRNA regimen were most affected after the first vaccination (Fig. 2d).

Mixing different vaccine types in heterologous regimens has already been deployed in previous vaccine studies. Examples include

---

Fig. 1 | Immune responses against the SARS-CoV-2 spike protein after vaccination with homologous and heterologous prime–booster regimens. Immune responses were compared between individuals who received either homologous ChAdOx1 nCoV-19 vector/vector vaccination (*n* = 55), heterologous ChAdOx1 nCoV-19 vector/mRNA vaccination (*n* = 96) or homologous mRNA/mRNA vaccination (*n* = 62). **a,b**, Spike-specific IgG levels (**a**) and neutralizing antibodies (ab) (**b**) were quantified by ELISA and a surrogate neutralization assay. **c,d**, Percentages of SARS-CoV-2 spike-specific (**c**) and SEB-reactive (**d**) CD4 and CD8 T cells were determined after antigen-specific stimulation of whole-blood samples, followed by intracellular cytokine analysis using flow cytometry. Reactive cells were identified by coexpression of CD69 and IFN-γ among CD4 or CD8 T cells and subtraction of background reactivity of respective negative controls. **e**, Correlations between spike-specific T cell levels, antibody responses and numbers of plasmablasts. **f**, Cytokine expression profiles of spike-specific CD4 and CD8 T cells in all individuals showing single or combined expression of IFN-γ, IL-2 and TNF-α (gating strategy shown in Extended Data Fig. 5). **a–d**, Bars represent medians with IQR. Individuals who received the mRNA-1273 vaccine are indicated in gray (1x vector/mRNA, 9x mRNA/mRNA). Differences between groups were calculated using a two-sided Kruskal–Wallis test with Dunn´s multiple comparisons post test. **e**, Correlation coefficients (*r*) were analyzed according to two-tailed Spearman (Supplementary Table 1). **f**, Bars represent means and standard deviation; ordinary one-way ANOVA tests were performed. **a,b**, Dotted lines indicate detection limits (DL) for antibodies, indicating negative, intermediate and positive levels or levels of inhibition, respectively, per the manufacturer's instructions. **c,d**, Dotted lines indicate detection limits for SARS-CoV-2-specific CD4 T cells. **f**, Analysis was restricted to samples with ≥30 cytokine-positive T cells (*n* = 31 (CD4) and *n* = 15 (CD8) for vector/vector, *n* = 89 and *n* = 73 for vector/mRNA and *n* = 58 and *n* = 24 for mRNA/mRNA).
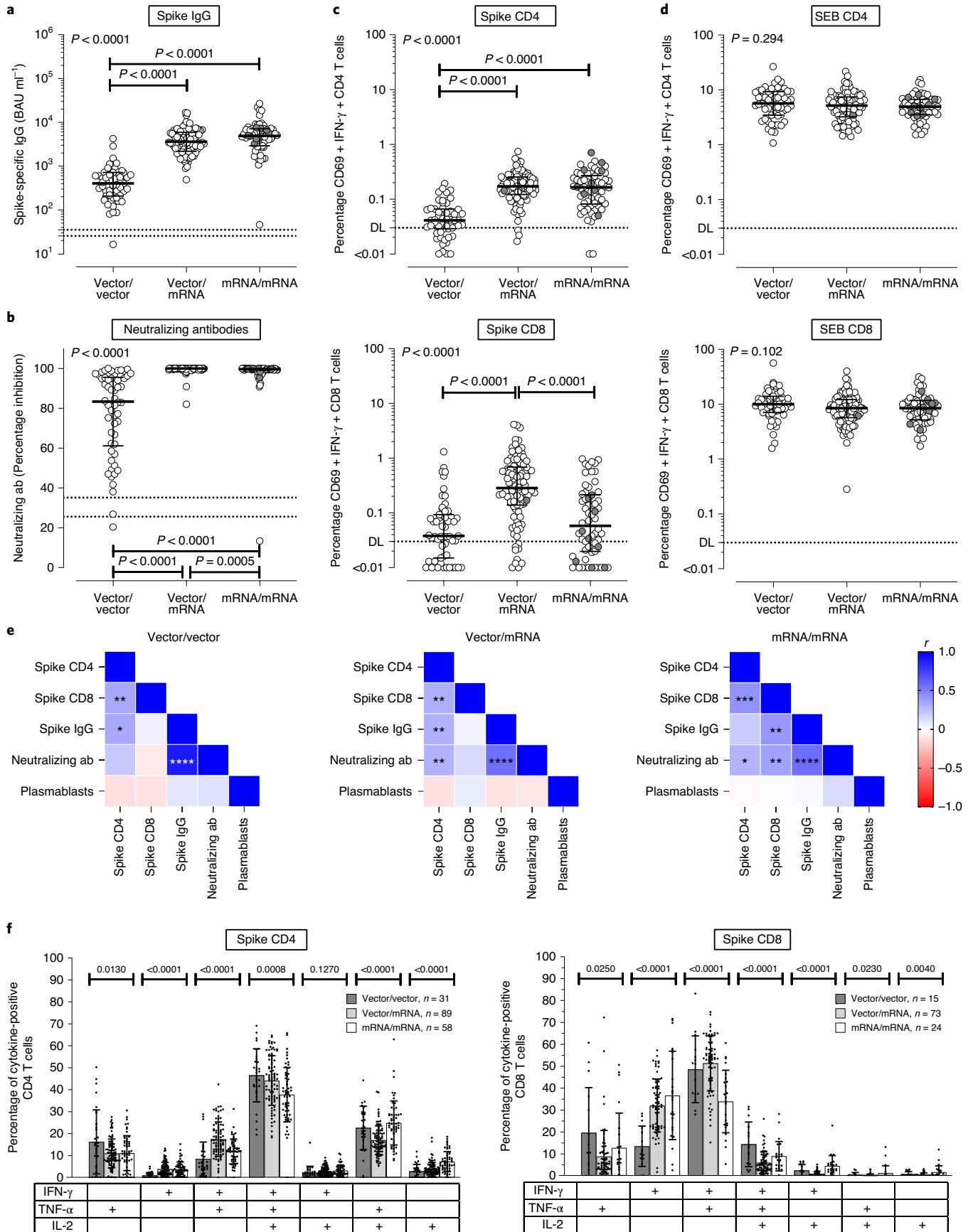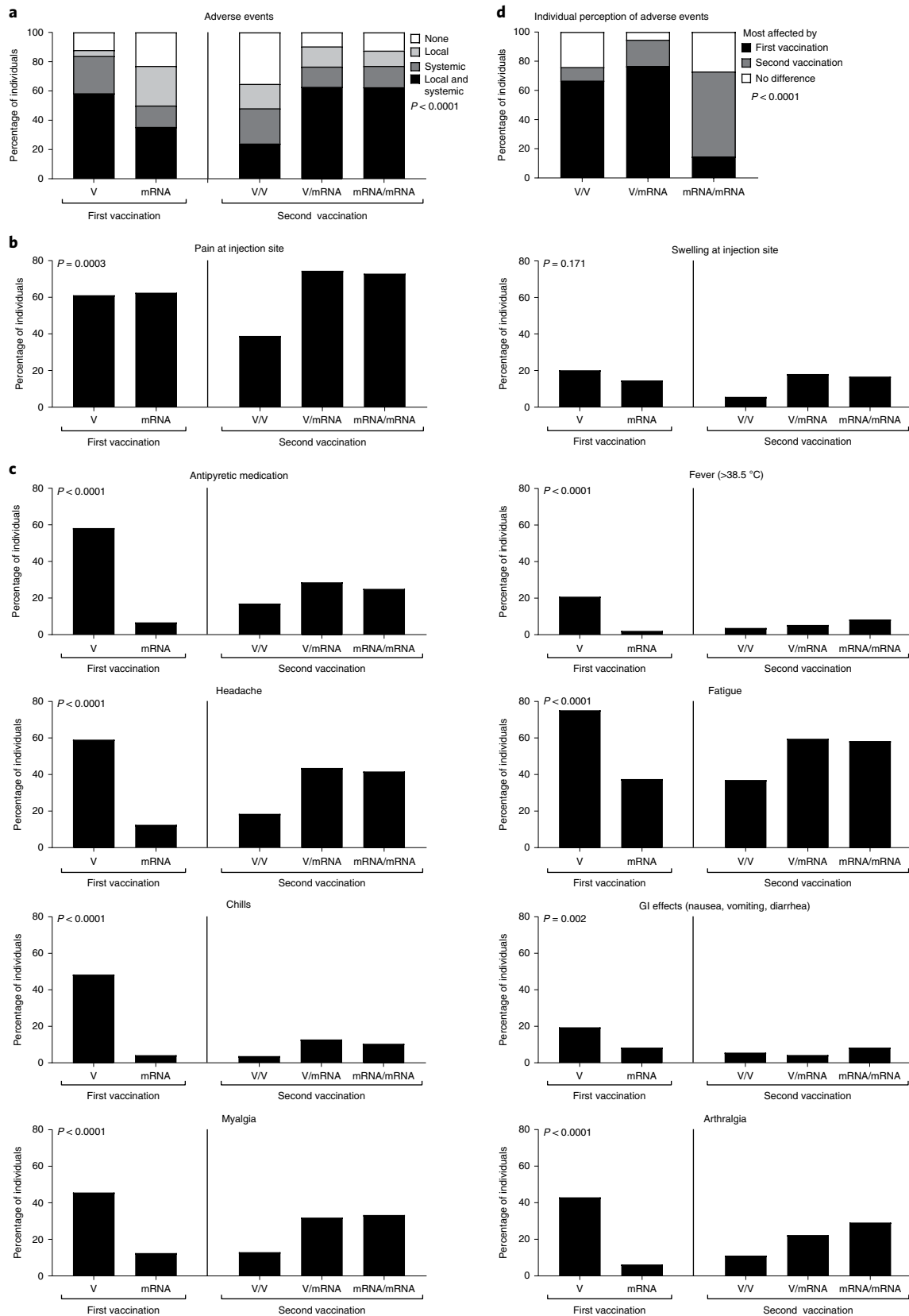
Fig. 2 | Reactogenicity after primary and secondary vaccination with homologous and heterologous prime–booster regimens. a–c, Reactogenicity within the first week after priming and after the booster dose was self-reported based on a standardized questionnaire, and was analyzed after the first vaccination with either vector (V, n = 150) or mRNA vaccine (mRNA, n = 48), and after the second vaccination with homologous (V/V, n = 54; mRNA/mRNA, n = 48) and heterologous (V/mRNA, n = 95) vaccine regimens with respect to local/systemic reactions in general (**a**), stratified for local (**b**) and various systemic adverse events (**c**). **d**, Individual perception of which of the two vaccinations had the greater affect. Comparisons between groups were performed using the X^2 test. GI, gastrointestinal.

experimental vaccines towards human immunodeficiency virus[8] and malaria[9], and the authorized vector vaccine against Ebola virus disease[10]. Although no data were available on the immunogenicity and efficacy of heterologous strategies among authorized COVID-19 vaccines, this raised confidence in recommending a heterologous mRNA booster vaccination in ChAdOx1 vector-primed individuals after recognition of severe adverse events of cerebral venous thrombosis[4,5]. We show that the heterologous regimen led to a strong induction of both antibodies and T cells. IgG levels were similar in magnitude to those following homologous mRNA vaccination, and approximately tenfold higher than those after homologous vector vaccination. Similar differences were found for vaccine-induced CD4 T cells, while neutralizing antibody activity and spike-specific CD8 T cell numbers were even more pronounced after heterologous vaccination. Similar results were recently reported in mice[11]. Despite the strong ability of the ChAdOx1 vaccine to induce T cells after priming[7], the strikingly lower immunogenicity following the homologous ChAdOx1 booster dose affected both antibodies and T cells. This may result from neutralizing immunity towards the vector backbone induced after the first vaccine dose[12], which could have rendered secondary vaccination less efficient. Our results show that both vector-primed antibodies and T cells are particularly well induced when combined with mRNA as the secondary vaccine.

Although the heterologous group reported more pronounced systemic adverse events after vector priming, boosting with the mRNA vaccine was less severe and well tolerated and the spectrum of both local and systemic adverse events was comparable to the homologous mRNA regimens. A recent study also showed strong induction of humoral immunity after a second dose of BNT162b2 in individuals primed with the vector vaccine. Similar to our study, the booster dose was given 8–12 weeks after priming[13]. Although there was no direct comparison with homologous regimens, the reactogenicity profile was also rather moderate[13]. This contrasts with reactogenicity data from the Com-COV trial, where adverse events in the heterologous regimens were more severe than in homologous groups[14]. Whether this was due to the shorter interval between priming and boosting (4 versus 9–12 weeks) and whether this affects immunogenicity await further study. Our observational study based on a convenience cohort is limited by the fact that direct comparison of immunity in the same individuals after the first vaccine dose was not possible, because data after primary vaccination were available for only a subset of the mRNA/mRNA group and the majority of vector-primed individuals were enrolled after primary vaccination. However, in a separate group of vector-primed individuals, antibody levels were higher following mRNA priming whereas T cell levels were higher after vector priming[7]. Another limitation of our study is that most mRNA vaccine recipients received BNT162b2, although results appear similar for mRNA-1273. In addition, the homologous ChAdOx1 nCoV-19 vaccine group was slightly older due to age-related differences in general recommendations. However, because a subgroup analysis of age-matched individuals gave the same results (Extended Data Fig. 7), we speculate that the difference in age is unlikely to account for the reduced immune responses in this group. Although we show strong neutralizing activity in a surrogate assay, neutralizing activity towards wild-type virus or variants of concern was not specifically assessed. Finally, no vaccine efficacy data are available to inform on protection from infection or disease. While this awaits further study, immune-based correlates of protection will be important in estimating the efficacy of vaccines and vaccine combinations[15]. Neutralizing antibodies have been discussed as promising candidates[15,16] that mirror the efficacy of vector and mRNA regimens[1–3]. Because immunogenicity after heterologous vaccination is comparable—or in part superior—to homologous mRNA regimens, it will be interesting to see whether this translates into similar efficacy.

Although vaccine development focuses on antibodies due to their ability to confer sterilizing immunity, T cells are important in mediating protection from severe disease[17] and may be less affected by virus variants[18]. The T cell data from this and similar studies could influence the development of future vaccine strategies, including how to improve vaccine-induced T cell immunity and protection from severe disease among vulnerable groups of immunocompromised patients.

Online content

Any methods, additional references, Nature Research reporting summaries, source data, extended data, supplementary information, acknowledgements, peer review information; details of author contributions and competing interests; and statements of data and code availability are available at https://doi.org/10.1038/s41591-021-01464-w.

References

1. Voysey, M. et al. Safety and efficacy of the ChAdOx1 nCoV-19 vaccine (AZD1222) against SARS-CoV-2: an interim analysis of four randomised controlled trials in Brazil, South Africa, and the UK. *Lancet* **397**, 99–111 (2021).
2. Baden, L. R. et al. Efficacy and safety of the mRNA-1273 SARS-CoV-2 vaccine. *N. Engl. J. Med.* **384**, 403–416 (2021).
3. Polack, F. P. et al. Safety and efficacy of the BNT162b2 mRNA Covid-19 Vaccine. *N. Engl. J. Med.* **383**, 2603–2615 (2020).
4. Greinacher, A. et al. Thrombotic thrombocytopenia after ChAdOx1 nCov-19 vaccination. *N. Engl. J. Med.* **384**, 2092–2101 (2021).
5. Schultz, N. H. et al. Thrombosis and thrombocytopenia after ChAdOx1 nCoV-19 vaccination. *N. Engl. J. Med.* **384**, 2124–2130 (2021).
6. Vygen-Bonnet, S. et al. Beschluss der STIKO zur 5. Aktualisierung der COVID-19-Impfempfehlung und die dazugehörige wissenschaftliche Begründung. *Epidemiol. Bull.* **19**, 24–36 (2021).
7. Schmidt, T. et al. Cellular immunity predominates over humoral immunity after the first dose of COVID-19 vaccines in solid organ transplant recipients. Preprint at https://www.medrxiv.org/content/10.1101/2021.05.07.21256809v1 (2021).
8. Rerks-Ngarm, S. et al. Vaccination with ALVAC and AIDSVAX to prevent HIV-1 infection in Thailand. *N. Engl. J. Med.* **361**, 2209–2220 (2009).
9. McConkey, S. J. et al. Enhanced T-cell immunogenicity of plasmid DNA vaccines boosted by recombinant modified vaccinia virus Ankara in humans. *Nat. Med.* **9**, 729–735 (2003).
10. Pollard, A. J. et al. Safety and immunogenicity of a two-dose heterologous Ad26.ZEBOV and MVA-BN-Filo Ebola vaccine regimen in adults in Europe (EBOVAC2): a randomised, observer-blind, participant-blind, placebo-controlled, phase 2 trial. *Lancet Infect. Dis.* **21**, 493–506 (2021).
11. Spencer, A. J. et al. Heterologous vaccination regimens with self-amplifying RNA and adenoviral COVID vaccines induce robust immune responses in mice. *Nat. Commun.* **12**, 2893 (2021).
12. Ramasamy, M. N. et al. Safety and immunogenicity of ChAdOx1 nCoV-19 vaccine administered in a prime-boost regimen in young and old adults (COV002): a single-blind, randomised, controlled, phase 2/3 trial. *Lancet* **396**, 1979–1993 (2021).
13. Borobia, A. M. et al. Immunogenicity and reactogenicity of BNT162b2 booster in ChAdOx1-S-primed participants (CombiVacS): a multicentre, open-label, randomised, controlled, phase 2 trial. *Lancet* **398**, 121–130 (2021).
14. Shaw, R. H. et al. Heterologous prime-boost COVID-19 vaccination: initial reactogenicity data. *Lancet* **397**, 2043–2046 (2021).
15. Kristiansen, P. A. et al. WHO International Standard for anti-SARS-CoV-2 immunoglobulin. *Lancet* **397**, 1347–1348 (2021).
16. Khoury, D. S. et al. Neutralizing antibody levels are highly predictive of immune protection from symptomatic SARS-CoV-2 infection. *Nat. Med.* https://doi.org/10.1038/s41591-021-01377-8 (2021).
17. Rydyznski Moderbacher, C. et al. Antigen-specific adaptive immunity to SARS-CoV-2 in acute COVID-19 and associations with age and disease severity. *Cell* **183**, 996–1012 (2020).
18. Skelly, D. T. et al. Vaccine-induced immunity provides more robust heterotypic immunity than natural infection to emerging SARS-CoV-2 variants of concern. Preprint at https://www.researchsquare.com/article/rs-226857/v1 (2021).

Methods

Study design and subjects. A convenience cohort of immunocompetent individuals with no known history of SARS-CoV-2 infection was invited to participate in this observational study, and were enrolled before secondary vaccination and after primary vaccination with either ChAdOx1 nCoV-19 or one of the mRNA vaccines (BNT162b2 or mRNA-1273). The majority of study participants were PCR tested on a regular basis due to their occupational activity in a hospital setting. This study was not a randomized clinical trial, but was based on the revised recommendations that were issued in Germany on 1 April 2021 for secondary vaccination of all individuals who had received the first dose of the ChAdOx1 nCoV-19 vector vaccine[6]. The study did not influence the decision on vaccine regimens: decisions were exclusively assigned based on current recommendations[6]. Blood sampling for immunological analyses was performed after having received a homologous vaccine regimen comprising either ChAdOx1 nCoV-19 or one of the mRNA vaccines (BNT162b2 or mRNA-1273), or a heterologous vaccine regimen comprising a ChAdOx1 nCoV-19 priming dose followed by secondary vaccination with an mRNA vaccine. The time interval between the first and second dose was determined as per national guidelines[6] and varied from 3 to 6 weeks for the homologous mRNA regimens to 9–12 weeks for the homologous ChAdOx1 nCoV-19 and the heterologous ChAdOx1 nCoV-19/mRNA regimena[19]. Lymphocyte subpopulations, as well as vaccine-induced SARS-CoV-2-specific humoral and cellular immunity, were determined from heparinized whole blood 14 days after the second vaccine dose, with an interval of 13–18 days tolerated. Local and systemic adverse events within 7 days after the first and second vaccination were self-reported using a standardized questionnaire. Reactogenicity after the second dose was collected prospectively in all cases using a standardized questionnaire. Reactogenicity data after the first dose were collected retrospectively in the majority of cases, but all participants felt confident in recalling adverse events at the time of enrollment into the study.

Vaccinations were performed between 10 January and 8 April 2021. All individuals in the vector-primed group had their first vaccination before 1 April, because primary vector vaccination was suspended at Saarland University Medical Center thereafter. Immunity after secondary vaccination in 28 individuals in the mRNA/mRNA group was tested before 1 April. Testing in these individuals was offered as a service to those working in intensive care units on a voluntary basis as part of routine diagnostics. All provided written informed consent to have their immunogenicity and reactogenicity data included as control group in this study. Moreover, 32 individuals (20 mRNA and 12 vector primed) represent a subgroup of immunocompetent controls enrolled in a separate observational study (SaarTxVac study). Their results following the induction of humoral and cellular immunity after the first vaccination are part of a separate manuscript[7] that addresses the induction of humoral and cellular immunity after vector and mRNA priming in immunocompetent individuals and transplant recipients. The results of their immune response after secondary vaccination (18 cases tested before and 14 after 1 April) are included in the present study. The study was approved by the ethics committee of the Ärztekammer des Saarlandes (no. 76/20), and all individuals gave written informed consent.

Quantification of lymphocyte populations and plasmablasts. T cells, B cells and plasmablasts were quantified from 100 µl of heparinized whole blood as described previously[20] using monoclonal antibodies towards CD3 (clone SK7, final dilution 1:25), CD19 (clone HIB19, 1:40), CD27 (clone L128, 1:200), CD38 (clone HB7, 1:20) and IgD (clone IA6-2, 1:33.3). T and B cells were identified among total lymphocytes by expression of CD3 and CD19, respectively. Plasmablasts were characterized by expression of CD38 among IgD⁻CD27⁺ CD19-positive switched-memory B cells. CD4 and CD8 T cells were quantified after additional staining of CD4 (clone SK3, 1:100) and CD8 (clone RPA-T8). Antibodies used are listed in Supplementary Table 2. Analysis was performed on a BD FACSLyric flow-cytometer and BD FACSuite software v.1.4.0.7047, followed by data analysis using FlowJo software 10.6.2. The gating strategy is shown in Supplementary Fig. 1. Absolute lymphocyte numbers were calculated based on differential blood counts.

Quantification of vaccine-induced SARS-CoV-2-specific T cells. SARS-CoV-2-specific T cells were determined from heparinized whole blood after 6-h stimulation with overlapping peptides spanning the SARS-CoV-2 spike protein (N-terminal receptor binding domain and C-terminal portion including the transmembrane domain, each peptide 2 µg ml⁻¹; JPT) as described previously[20]. Stimulations with 0.64% DMSO and 2.5 µg ml⁻¹ of SEB (Sigma) served as negative and positive controls, respectively. All stimulations were carried out in the presence of costimulatory antibodies against CD28 and CD49d (clones L293 and 9F10, 1 µg ml⁻¹ each). Immunostaining was performed using anti-CD4 (clone SK3, 1:33.3), anti-CD8 (clone SK1, 1:12.5), anti-CD69 (clone L78, 1:33.3), anti-IFN-γ (clone 4 S.B3, 1:100), anti-IL-2 (clone MQ1-17H12, 1:12.5) and anti-TNF-α (clone MAb11, 1:20), and analyzed using flow cytometry (BD FACS Canto II, including BD FACSdiva software 6.1.3). Antibodies are listed in Supplementary Table 2. SARS-CoV-2-reactive CD4 or CD8 T cells were identified as activated CD69-positive T cells producing IFN-γ (see Extended Data Fig. 3 for gating

strategy). Moreover, coexpression of IL-2 and TNF-α was analyzed to characterize cytokine expression profiles. Reactive CD4 and CD8 T cell levels after control stimulations were subtracted from those obtained after SARS-CoV-2-specific stimulation, and 0.03% of reactive T cells was set as the detection limit based on the distribution of T cell frequencies after control stimulations.

Determination of SARS-CoV-2-specific antibodies and neutralization capacity. SARS-CoV-2-specific IgG antibodies towards the receptor binding domain of SARS-CoV-2 spike protein were quantified using an enzyme-linked immunosorbent assay (ELISA) according to the manufacturer's instructions (SARS-CoV-2-QuantiVac, Euroimmun). Antibody binding units (BAU ml⁻¹) <25.6 were scored negative, ≥25.6 and <35.2 were scored intermediate and ≥35.2 were scored positive. SARS-CoV-2-specific IgGs towards the N protein were quantified using ELISA according to the manufacturer´s instructions (Anti-SARS-CoV-2-NCP-ELISA, Euroimmun). Antibody levels are calculated as ratios defined as the extinction of the patient sample divided by the extinction of a calibrator serum. Ratios ≥1.1 were scored positive. A neutralization assay based on antibody-mediated inhibition of soluble ACE2 binding to the plate-bound S1 receptor binding domain was used at a single serum dilution according to the manufacturer's instructions (SARS-CoV-2-NeutraLISA, Euroimmun). Surrogate neutralizing capacity was calculated as percentage of inhibition (IH) by 1 minus the ratio of the extinction of the respective sample and the extinction of the blank value. IH < 20% was scored negative, IH ≥ 20 to <35 intermediate and IH ≥ 35% positive.

Statistical analysis. Kruskal–Wallis testing, followed by Dunn's multiple comparisons test, was performed to compare unpaired nonparametric data between groups (lymphocyte subpopulations, T cell and antibody levels). Data with normal distribution were analyzed using ordinary one-way analysis of variance (cytokine expression profiles, age). Categorial analyses on gender and adverse events were performed using the X^2 test. Correlations between levels of T cells, antibodies and plasmablasts were analyzed according to Spearman, and $P < 0.05$ was considered statistically significant. Analysis was carried out using GraphPad Prism 9.0 software using two-tailed tests. Cytokine profiles were plotted using the VennDiagram package (v.1.6.20)[21] running under R (v.4.0.2).

Reporting Summary. Further information on research design is available in the Nature Research Reporting Summary linked to this article.

Data availability

Figures 1 and 2 and Extended Data Figs. 2 and 4–7 have associated raw data. The data that support the findings of this study are available from the corresponding author upon request, and data are available in a public repository (https://doi.org/10.5281/zenodo.5080642). Because age and the individual assignment of the mRNA vaccine (BNT162b2 or mRNA-1273) may be subject to confidentiality, data in the repository refer to age groups, and mRNA vaccines are not specified individually.

References

19. Vygen-Bonnet, S. et al. Beschluss der STIKO zur 3. Aktualisierung der COVID-19-Impfempfehlung und die dazugehörige wissenschaftliche Begründung. *Epidemiol. Bull.* **12**, 13–25 (2021).
20. Schub, D. et al. High levels of SARS-CoV-2-specific T cells with restricted functionality in severe courses of COVID-19. *JCI Insight* **5**, e142167 (2020).
21. Chen, H. & Boutros, P. C. VennDiagram: a package for the generation of highly-customizable Venn and Euler diagrams in R. *BMC Bioinformatics* **12**, 35 (2011).

Author contributions

T.S., D.S., U.S., B.C.G., S.S. and M.S. designed the study. T.S., D.S., U.S. and M.S. designed the experiments. V.K., F.H., S.M., A.A.-O., L.Z., C.G., R.U. and T.S. performed experiments. S.S., B.C.G., J.M., L.Z., S.L.B. and U.S. contributed to study design, patient recruitment and clinical data acquisition. D.S., V.K., T.S., U.S., J.M. and M.S. supervised all parts of the study, performed analyses and wrote the manuscript. All authors approved the final version of the manuscript.

Competing interests

M.S. has received grant support from Astellas and Biotest to the organization Saarland University outside the submitted work, and honoraria for lectures from Biotest and Novartis. All other authors of this paper have no conflicts of interest.
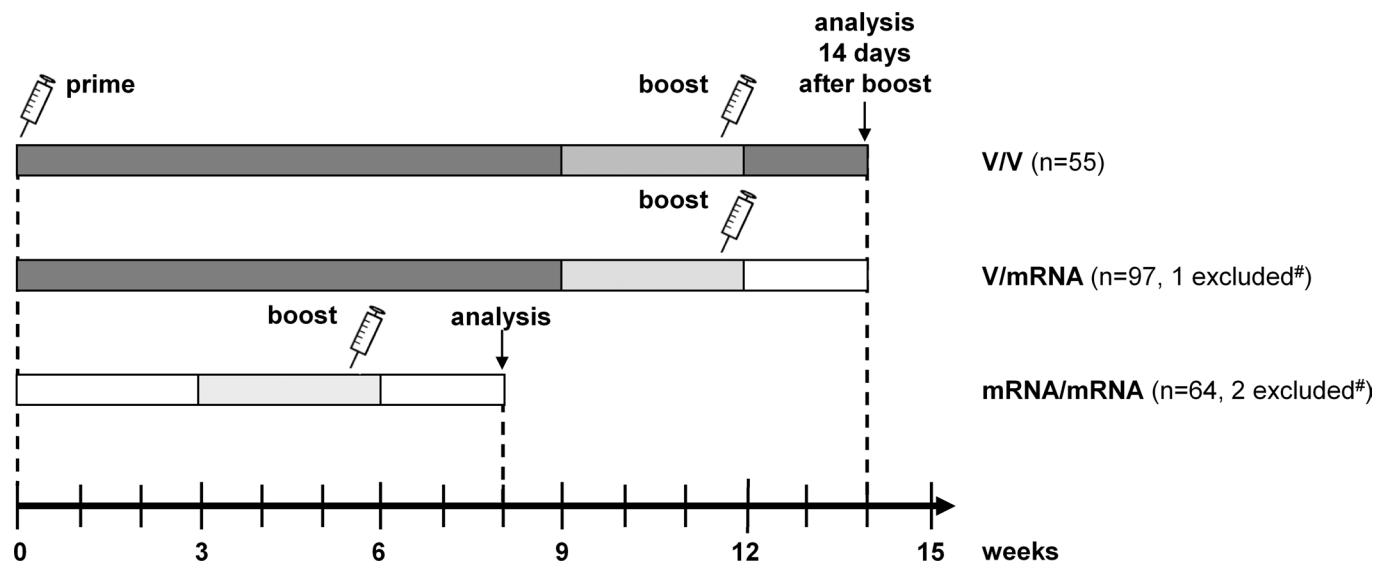
Additional information

Extended Data Fig. 1 | Study design. Time between first and second vaccination and the time between second vaccination and analysis is shown for the three vaccination regimens (homologous ChAdOx1 nCoV-19 vector vaccination (V/V, n=55), heterologous ChAdOx1 nCoV-19 vector/mRNA vaccination (V/mRNA, n=97) or homologous mRNA vaccination (mRNA/mRNA, n=64). #3 individuals were excluded from further analysis due to IgG positivity in a SARS-CoV-2 nucleocapsid ELISA.

## Demographic and clinical characteristics of the study population

1° vaccine	Vector	Vector	mRNA	
2° vaccine	vector[1]	mRNA[2]	mRNA[3]	
	n=55	n=96	n=62	p-value
Years of age (mean±SD)	48.6±11.9	40.8±11.1	44.7±14.3	0.001[§]
Female gender, n (%)	35 (63.6)	70 (72.9)	44 (71.0)	0.478[†]
Weeks between 1° and 2° vaccination, (mean±SD)	10.8±1.4	11.2±1.3	4.3±1.1	
Analysis time [days after 2° vaccination], median (IQR)	14 (2)	14 (1)	14 (1.25)	
Differential blood cell counts	n=55	n=96	n=60	
Leukocytes (cells/µl), median (IQR)	6800 (2500)	6900 (2150)	6900 (2275)	0.994[‡]
Granulocytes (cells/µl), median (IQR)	4057 (1829)	3925 (1812)	3867 (1757)	0.921[‡]
Monocytes (cells/µl), median (IQR)	590 (238)	545 (256)	555 (180)	0.244[‡]
Lymphocytes (cells/µl), median (IQR)	2291 (840)	2232 (713)	2212 (793)	0.999[‡]
CD3 T-cells (cells/µl), median (IQR)[#]	1565 (603)	1589 (639)	1559 (878)	0.924[‡]
CD4 T-cells (cells/µl), median (IQR)[#]	1000 (450)	974 (389)	1065 (615)	0.407[‡]
CD8 T-cells (cells/µl), median (IQR)[#]	394 (282)	431 (236)	378 (274)	0.297[‡]
CD19 B cells (cells/µl), median (IQR)[#]	218 (193)	203 (141)	200 (142)	0.758[‡]
Plasmablasts (cells/µl), median (IQR)[#]	0.414 (0.512)	0.416 (0.479)	0.452 (0.683)	0.464[‡]

[1]55x ChAdOx1 nCoV-19; [2]95x BNT162b2, 1x mRNA-1273; [3]53x BNT162b2, 9x mRNA-1273; [§]Ordinary one-way ANOVA with Tukey's multiple comparisons test (p=0.0006 between Vector/Vector and Vector/mRNA); [†]X[2] test; [‡]two-sided Kruskal-Wallis test; [#]Plasmablasts, B and T-cell counts were calculated on 55 vector-vector, 96 vector-mRNA and 34 mRNA-mRNA vaccinated individuals, CD4 and CD8 T-cell counts in subgroups of 55, 96 and 16 individuals, respectively.

Extended Data Fig. 2 | Demographic and clinical characteristics of the study population. Demographic characteristics and vaccine-related data are shown for the three vaccination regimens (homologous ChAdOx1 nCoV-19 vector vaccination (V/V, n = 55), heterologous ChAdOx1 nCoV-19 vector/mRNA vaccination (V/mRNA, n = 96) or homologous mRNA vaccination (mRNA/mRNA, n = 62)). In addition, information on differential blood counts and on lymphocyte subpopulations is provided.
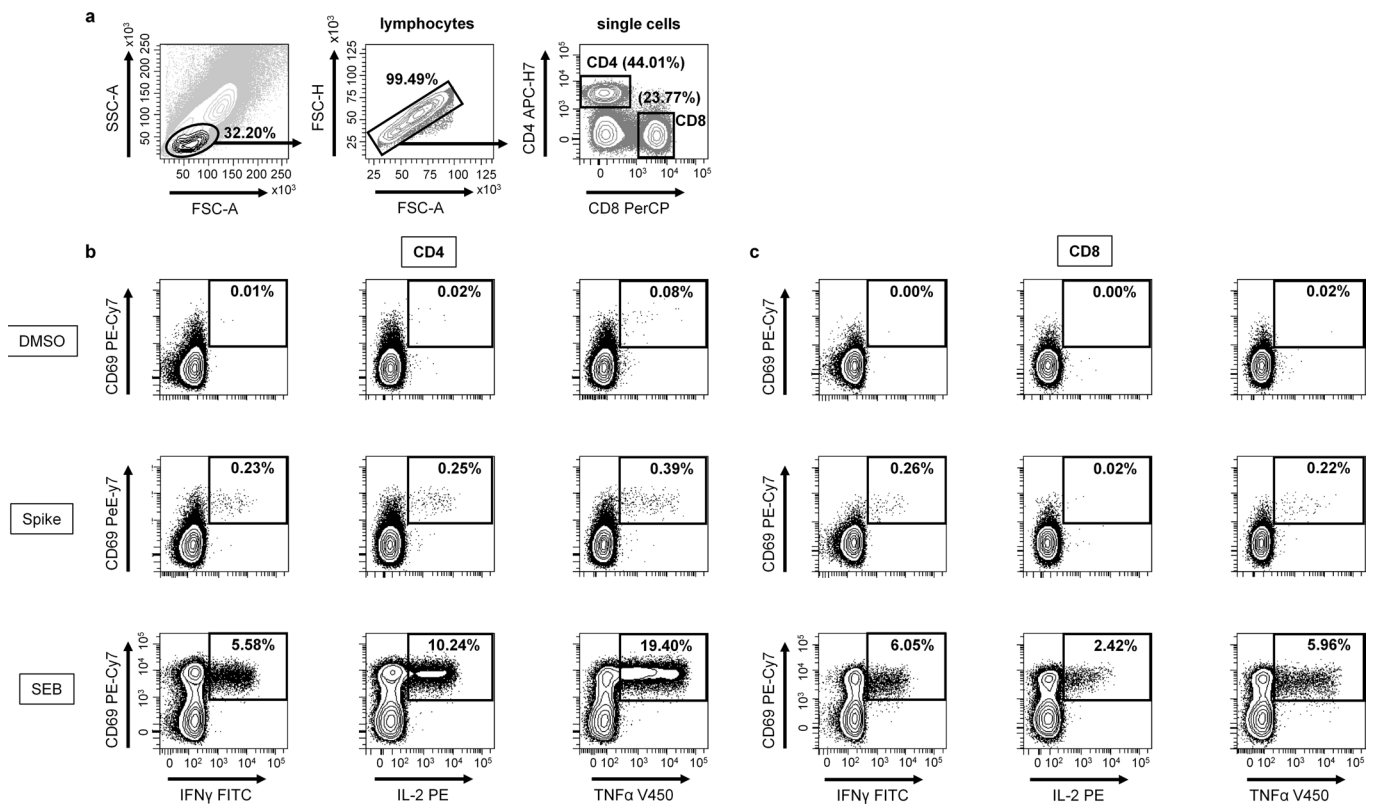
Extended Data Fig. 3 | Representative analysis of spike- and SEB-reactive CD4 and CD8 T cells. Lymphocytes were identified among total events by backgating of CD4 and/or CD8 positive cells combined with signals for size (FSC) and granularity (SSC). Hight and area signals of FSC were used to exclude doublets. CD4 T cells were identified among single cells by CD4 positive and CD8 negative signals. Likewise, CD8 T cells were defined as T cells being CD8 positive and CD4 negative. In (**b**) and (**c**) representative contour plots of CD4 and CD8 T cells of a 37-year-old female are shown after antigen-specific stimulation with SARS-CoV-2 spike peptides or respective control stimuli for negative (DMSO) or positive control (SEB) stimulation. Numbers indicate percentages of CD4 or CD8 T cells co-expressing the activation marker CD69 and the cytokines IFN-γ, IL-2 and/or TNF-α. FSC, forward scatter; IFN, interferon; IL, interleukin; SEB, Staphylococcus aureus enterotoxin B; SSC, side scatter; TNF, tumor necrosis factor.
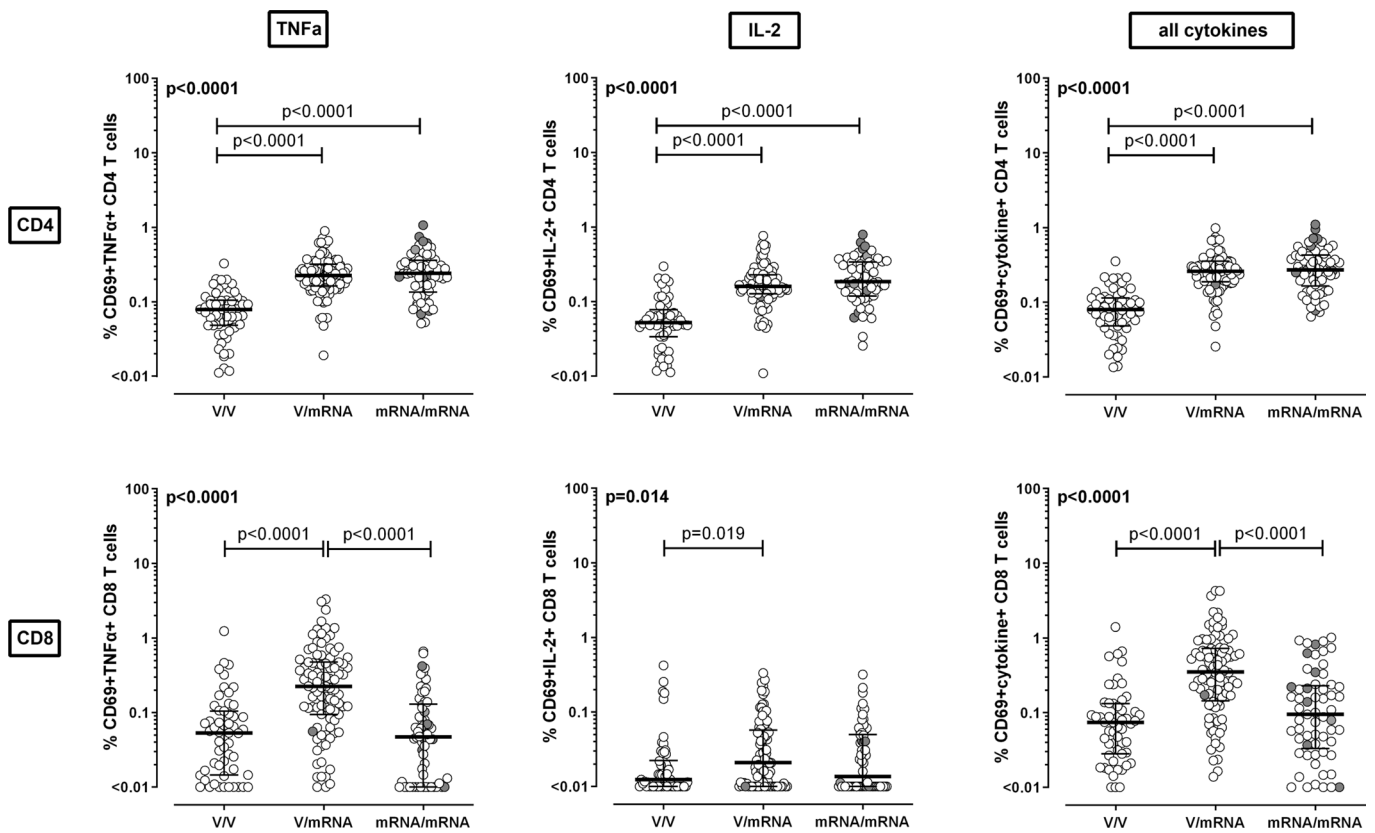
Extended Data Fig. 4 | SARS-CoV-2 spike-specific T cells producing TNF-α and IL-2 after vaccination with homologous and heterologous prime-booster regimens. Percentages of SARS-CoV-2 spike-specific CD4 and CD8 T cells were determined after antigen-specific stimulation of whole blood samples followed by intracellular cytokine analysis using flow-cytometry. Reactive cells were identified by co-expression of the activation marker CD69 and the cytokine tumor necrosis factor (TNF) α (left panel), interleukin 2 (IL-2, middle panel), or any of the cytokines analyzed (IFN-γ/TNF-α/IL-2, right panel), respectively, among CD4 or CD8 T cells and subtraction of background reactivity of respective negative control stimulations. T cell responses were compared between individuals who either received SARS-CoV-2 vector/vector (V/V, n = 55), vector/mRNA (V/mRNA, n = 96) or mRNA/mRNA vaccines (mRNA/mRNA, n = 62) using two-sided Kruskal-Wallis test with Dunn's multiple comparisons post test. Bars represent medians with interquartile ranges, individuals who received the mRNA-1273 vaccine are indicated by grey symbols.

a

b
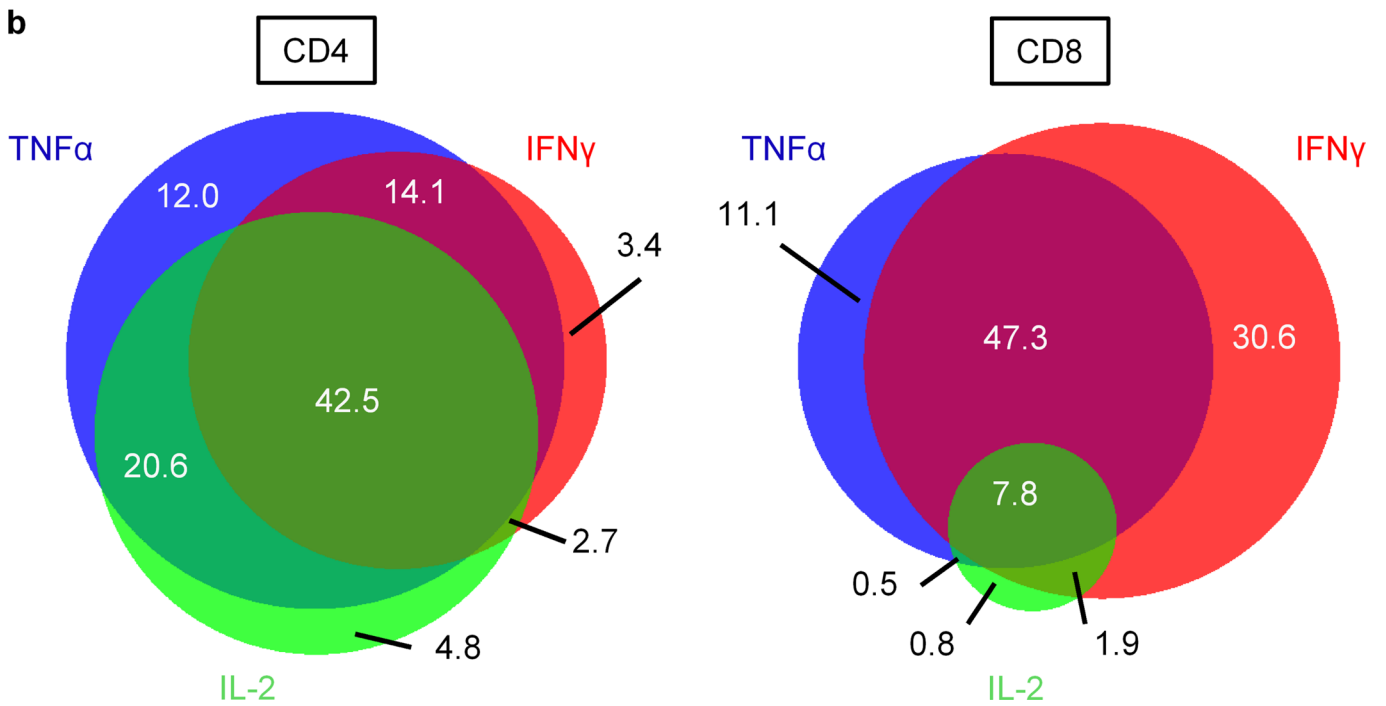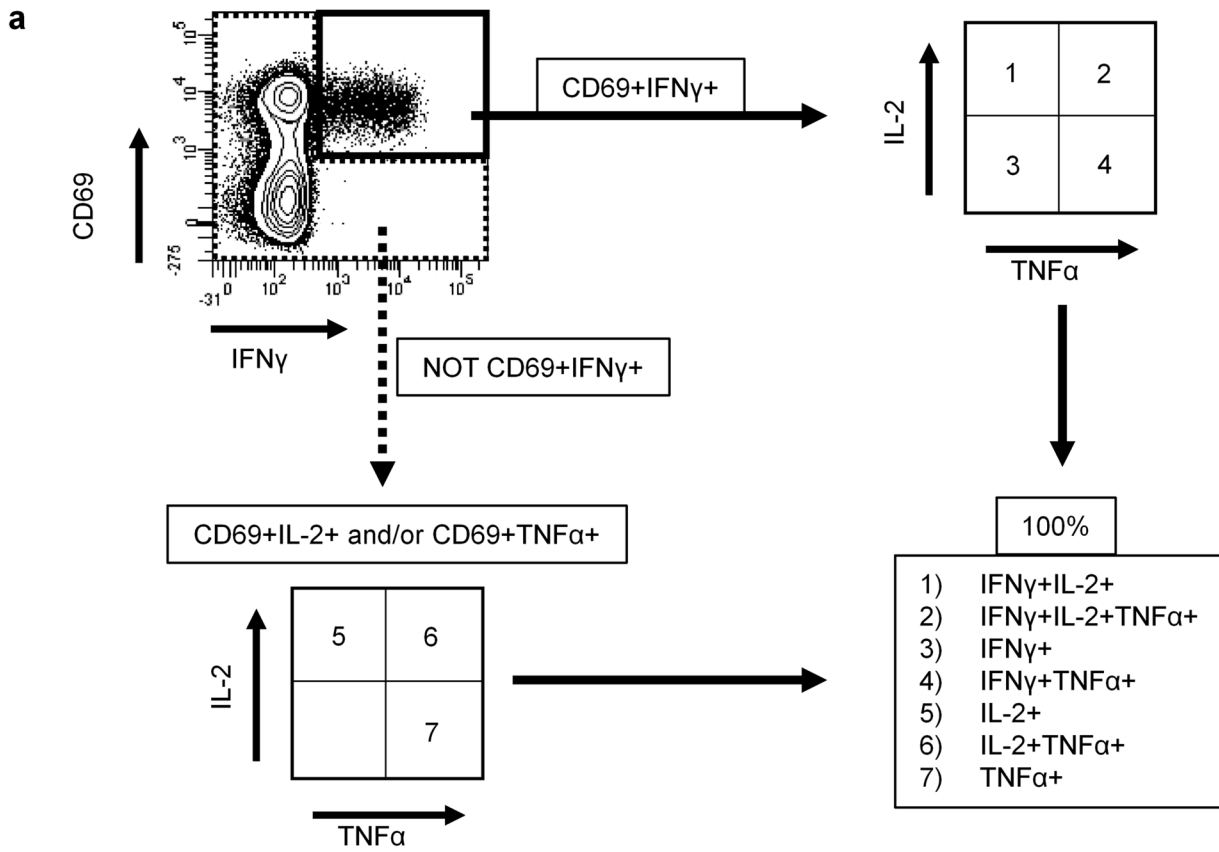
Extended Data Fig. 5 | See next page for caption.

Extended Data Fig. 5 | Gating strategy and analysis of spike-specific cytokine-expression profiles. (**a**) To characterize spike- and SEB-reactive CD4 T cells regarding their single or combined expression of the cytokines IFN-γ, IL-2, and TNF-α, CD4 T cells positive for combined expression of CD69 and IFN-γ were divided into four subpopulations according to additional expression of IL-2 and TNF-α. Using NOT Boolean Gating, all CD4 T cells which were not CD69 + IFN-γ + were analyzed for CD69 + IL-2+ and CD69 + TNF-α + CD4 T cells. Using OR Boolean Gating, CD69 + IL-2+ and/or CD69 + TNF-α + CD4 T cells were divided into IL-2 single, TNF-α single or IL-2+TNF-α + cells. After subtraction of background reactivity from negative control stimulations, the sum of these 7 subpopulations was set to 100%. A similar strategy was applied for CD8 T cells. (**b**) Cytokine-expression profiles of spike-specific CD4 and CD8 T cells in all individuals showing single or combined expression of the cytokines IFN-γ, interleukin (IL) 2 and tumor necrosis factor (TNF) α. To allow for robust statistics, analysis was restricted to samples with at least 30 cytokine-positive T cells (n = 178 for CD4 and n = 112 for CD8 T cells). Numbers refer to the percentage of cells expressing the respective cytokine. IFN, interferon; IL, interleukin; TNF, tumor necrosis factor.
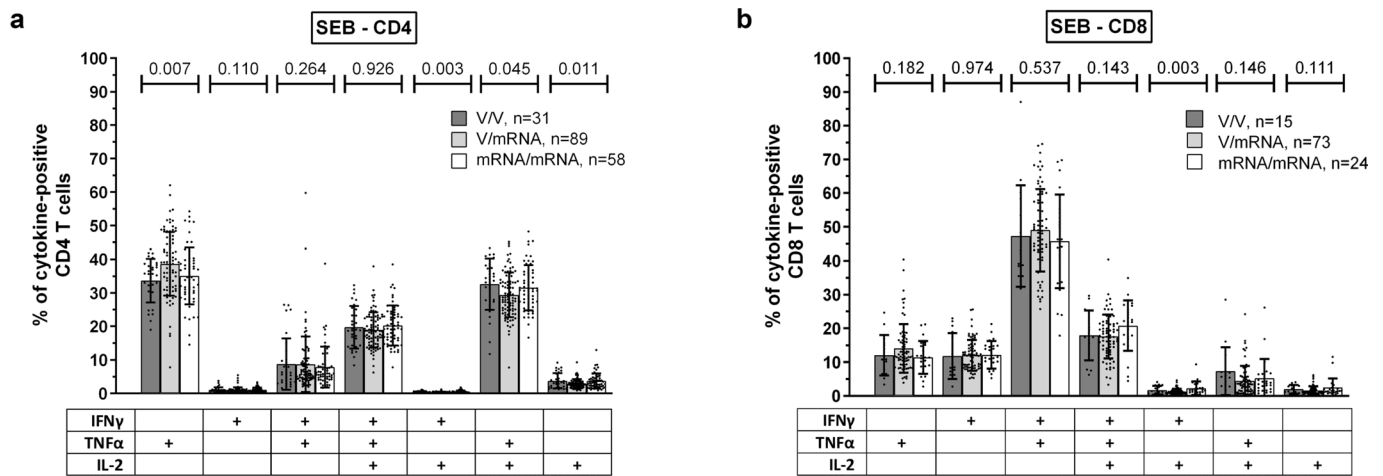
Extended Data Fig. 6 | Cytokine-expression profiles of SEB-reactive CD4 and CD8 T cells after vaccination with homologous and heterologous prime-booster regimens. Cytokine expression of CD4 (**a**) and CD8 T cells (**b**) after stimulation with Staphylococcus aureus enterotoxin B (SEB), was compared between individuals who either received SARS-CoV-2 vector/vector (V/V), vector/mRNA (V/mRNA), or mRNA/mRNA vaccine combinations. Cytokine-expressing T-cells were divided into 7 subpopulations according to their expression of IFN-γ, IL-2, and TNF-α (single, double or triple cytokine-expressing cells, for gating strategy, see Extended Data Fig. 5). Only samples of the study participants included in Fig. 1f are displayed (at least 30 cytokine-expressing CD4 or CD8 T-cells, respectively, after spike-specific stimulation, n = 31 and n = 15 for V/V, n = 89 and n = 73 for V/mRNA and n = 58 and n = 24 for mRNA/mRNA vaccine regimes). Differences among subpopulations between the groups were determined using ordinary one-way ANOVA test. Bars represent means and standard deviations of subpopulations among all SEB-reactive CD4 and CD8 T cells, respectively. IFN, interferon, IL, interleukin, TNF, tumor necrosis factor.
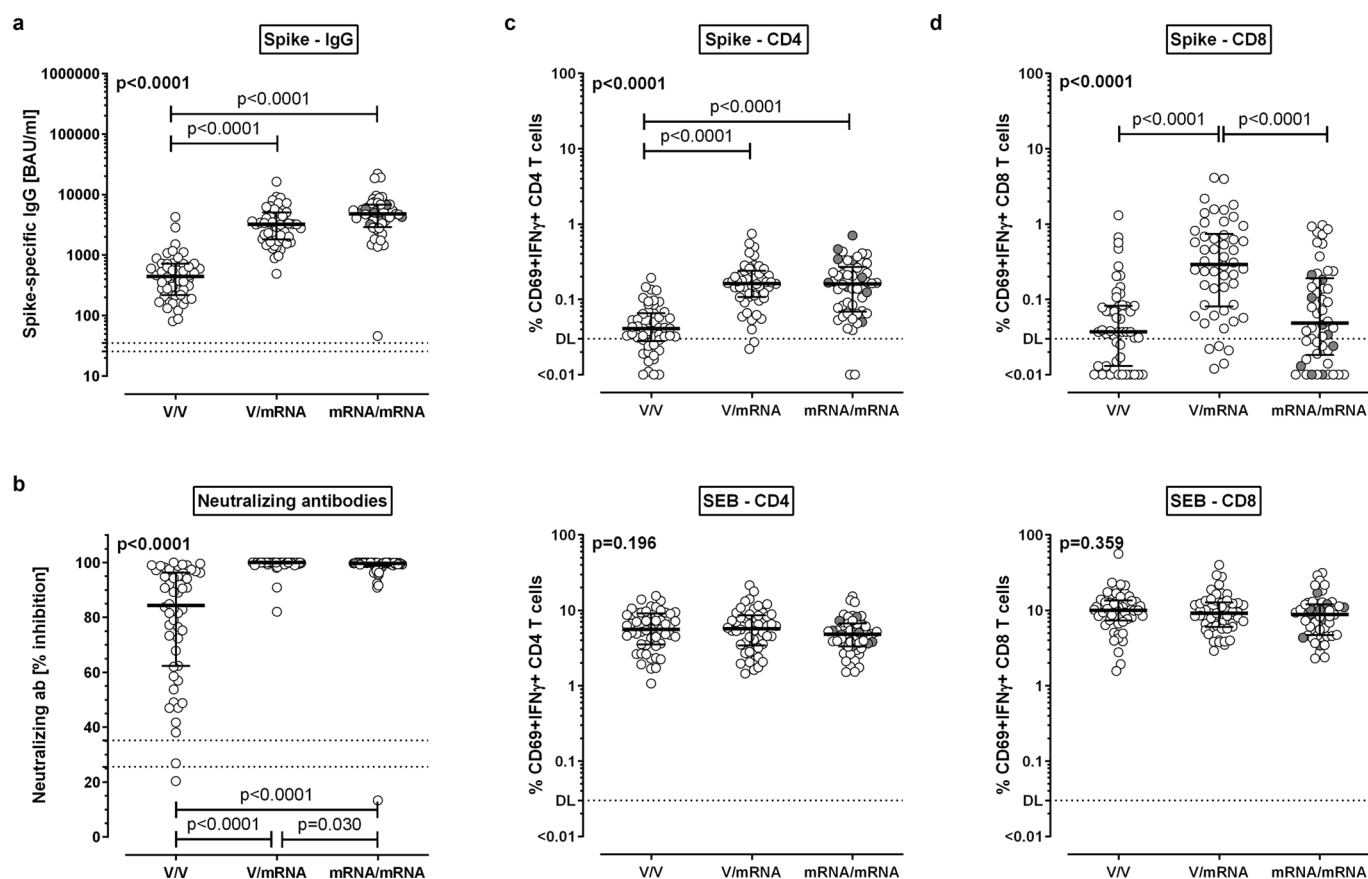
Extended Data Fig. 7 | Immune responses against the SARS-CoV-2 spike protein after vaccination with homologous and heterologous prime-booster regimens in age-matched subgroups. Immune responses were compared between age-matched subgroups of 50 individuals each who either received homologous ChAdOx1 nCoV-19 vector vaccination (V/V, mean age 47.0 ± 11.2 years, 33 females), heterologous ChAdOx1 nCoV-19 vector/mRNA vaccination (V/mRNA, 47.1 ± 9.2 years, 38 females) or homologous mRNA vaccination (mRNA/mRNA, 46.4 ± 11.5 years, 35 females, $p = 0.940$). Spike-specific IgG-levels (**a**) and neutralizing antibodies (**b**) were quantified by ELISA and a surrogate neutralization assay and compared between groups. Percentages of SARS-CoV-2 spike-specific (**c**) and SEB-reactive (**d**) CD4 and CD8 T cells were determined after antigen-specific stimulation of whole blood samples followed by intracellular cytokine analysis using flow-cytometry. Reactive cells were identified by co-expression of CD69 and the cytokine interferon (IFN) γ among CD4 or CD8 T cells and subtraction of background reactivity of respective negative control stimulations. Bars represent medians with interquartile ranges. Individuals who received the mRNA-1273 vaccine are indicated by grey symbols (9 in the homologous mRNA/mRNA group). Differences between the groups were calculated using two-sided Kruskal-Wallis test with Dunn´s multiple comparisons post test. Dotted lines indicate detection limits for antibodies in (a) and (b), indicating negative, intermediate and positive levels or levels of inhibition, respectively as per manufacturer's instructions, and detection limits for SARS-CoV-2-specific CD4 T cells in (c) and (d). SEB, Staphylococcus aureus enterotoxin B.

nature portfolio

Corresponding author(s):   Martina Sester

Last updated by author(s):   Jul 8, 2021

Reporting Summary

Nature Portfolio wishes to improve the reproducibility of the work that we publish. This form provides structure for consistency and transparency in reporting. For further information on Nature Portfolio policies, see our Editorial Policies and the Editorial Policy Checklist.

Statistics

For all statistical analyses, confirm that the following items are present in the figure legend, table legend, main text, or Methods section.

n/a	Confirmed	
☐	☒	The exact sample size (*n*) for each experimental group/condition, given as a discrete number and unit of measurement
☐	☒	A statement on whether measurements were taken from distinct samples or whether the same sample was measured repeatedly
☐	☒	The statistical test(s) used AND whether they are one- or two-sided *Only common tests should be described solely by name; describe more complex techniques in the Methods section.*
☒	☐	A description of all covariates tested
☒	☐	A description of any assumptions or corrections, such as tests of normality and adjustment for multiple comparisons
☐	☒	A full description of the statistical parameters including central tendency (e.g. means) or other basic estimates (e.g. regression coefficient) AND variation (e.g. standard deviation) or associated estimates of uncertainty (e.g. confidence intervals)
☐	☒	For null hypothesis testing, the test statistic (e.g. F, t, r) with confidence intervals, effect sizes, degrees of freedom and P value noted *Give P values as exact values whenever suitable.*
☒	☐	For Bayesian analysis, information on the choice of priors and Markov chain Monte Carlo settings
☒	☐	For hierarchical and complex designs, identification of the appropriate level for tests and full reporting of outcomes
☒	☐	Estimates of effect sizes (e.g. Cohen's *d*, Pearson's *r*), indicating how they were calculated

Our web collection on statistics for biologists contains articles on many of the points above.

Software and code

Policy information about availability of computer code

Data collection	BD FACSdiva software 6.1.3 BD FACSuite software v1.4.0.7047
Data analysis	BD FACSdiva software 6.1.3 FlowJo software 10.6.2 GraphPad Prism software 9.0 VennDiagram package version 1.6.20 running under R software version 4.0.2

For manuscripts utilizing custom algorithms or software that are central to the research but not yet described in published literature, software must be made available to editors and reviewers. We strongly encourage code deposition in a community repository (e.g. GitHub). See the Nature Portfolio guidelines for submitting code & software for further information.

Data

Policy information about availability of data

All manuscripts must include a data availability statement. This statement should provide the following information, where applicable:
- Accession codes, unique identifiers, or web links for publicly available datasets
- A description of any restrictions on data availability
- For clinical datasets or third party data, please ensure that the statement adheres to our policy

Figures 1, 2, and Extended Data figures 2, 4, 5, 6, and 7 have associated raw data. The data that support the findings of this study are available from the corresponding author upon request and data are available in a public repository (https://zenodo.org/record/5080642). As age and the individual assignment of the

mRNA vaccine (BNT162b2 or mRNA-1273) may be subject to confidentiality, data in the repository refer to age groups, and mRNA vaccines are not specified individually.

Field-specific reporting

Please select the one below that is the best fit for your research. If you are not sure, read the appropriate sections before making your selection.

☒ Life sciences   ☐ Behavioural & social sciences   ☐ Ecological, evolutionary & environmental sciences

For a reference copy of the document with all sections, see nature.com/documents/nr-reporting-summary-flat.pdf

Life sciences study design

All studies must disclose on these points even when the disclosure is negative.

Sample size	observational study with sample size according to availability, real-world recruitment of vaccinated individual at Saarland University Medical campus (convenience sampling).
Data exclusions	Data from 3 individuals with positive NCAP-IgG ratios were excluded from analyses.
Replication	Experimental procedures were pre-established before. Sufficient cells and plasma volumes were available to be analysed on each sample. Within each sample, no replicates were performed due to limited sample material.
Randomization	not applicable; individuals were recruited in an observational study with convenience samples being collected.
Blinding	Individuals were recruited on the various regimens. During sample processing and analysis of primary data, the investigators were blinded to vaccine group allocation.

Reporting for specific materials, systems and methods

We require information from authors about some types of materials, experimental systems and methods used in many studies. Here, indicate whether each material, system or method listed is relevant to your study. If you are not sure if a list item applies to your research, read the appropriate section before selecting a response.

Materials & experimental systems

n/a	Involved in the study
☐	☒ Antibodies
☒	☐ Eukaryotic cell lines
☒	☐ Palaeontology and archaeology
☒	☐ Animals and other organisms
☐	☒ Human research participants
☒	☐ Clinical data
☒	☐ Dual use research of concern

Methods

n/a	Involved in the study
☒	☐ ChIP-seq
☐	☒ Flow cytometry
☒	☐ MRI-based neuroimaging

Antibodies

Antibodies used	anti-CD3 mouse anti-human (BD Biosciences, PerCP, clone SK7, cat. 345766, Dilution 1:25) anti-CD4 mouse anti-human (BD Biosciences, APC-H7, clone SK3, cat. 641398, Dilution 1:100 for unstimulated samples and 1:33.3 for stimulated samples) anti-CD8 mouse anti-human (BD Biosciences, V500, clone RPA-T8, cat. 560774, Dilution 1:100) anti-CD8 mouse anti-human (BD Biosciences, PerCP, clone SK1, cat. 345774, Dilution 1:12.5) anti-CD19 mouse anti-human (BD Biosciences, FITC, clone HIB19, cat. 555412, Dilution 1:40) anti-CD27 mouse anti-human (BD Biosciences, APC, clone L128, cat. 337169, Dilution 1:200) anti-CD28 mouse anti-human (BD Biosciences, purified, clone L293, cat. 348040, 1μg/ml) anti-CD38 mouse anti-human (BD Biosciences, PE, clone HB7, cat. 345806, Dilution 1:20) anti-CD49d mouse anti-human (BD Biosciences, purified, clone 9F10, cat. 555501, 1μg/ml) anti-CD69 mouse anti-human (BD Biosciences, PE-Cy7, clone L78, cat. 335792, Dilution 1:33.3) anti-IFNγ mouse anti-human (BD Biosciences, FITC, clone 4S.B3, cat. 554551, Dilution 1:100) anti-IgD mouse anti-human (BD Biosciences, PE-Cy7, clone IA6-2, cat. 561314, Dilution 1:33.3) anti-IL-2 rat anti-human (BD Biosciences, PE, clone MQ1-17H12, cat. 559334, Dilution 1:12.5) anti-TNFα mouse anti-human (BD Biosciences, V450, clone Mab11, cat. 561311, Dilution 1:20)
Validation	All antibodies were separately titrated in house to evaluate best concentrations for discrimination of negative and positive cells. Finally, panels including defined concentration of antibodies were tested together to confirm that identified antibody concentrations are also sufficient when compensations are required.

SK7: CD3 is intended for in vitro diagnostic use in the identification of cells expressing the CD3 antigen. Application: Flow cytometry; Source: https://www.bdbiosciences.com/en-de/products/reagents/flow-cytometry-reagents/clinical-diagnostics/single-color-antibodies-asr-ivd-ce-ivd/cd3-percp.345766

SK3: The CD4 antibody, clone SK3, is derived from the hybridization of mouse NS-1 myeloma cells with spleen cells from BALB/c mice immunized with human peripheral blood T lymphocytes. The CD4 antibody recognizes a 55-kilodalton (kDa) glycoprotein that is present on T-helper/inducer lymphocytes and monocytes. Application: Flow cytometry; Source: https://www.bdbiosciences.com/en-de/products/reagents/flow-cytometry-reagents/clinical-discovery-research/single-color-antibodies-ruo-gmp/apc-h7-mouse-anti-human-cd4.641398

RPA-T8: The RPA-T8 monoclonal antibody specifically binds to CD8 alpha (CD8α). CD8α is a type I transmembrane glycoprotein and a member of the immunoglobulin superfamily. CD8α is expressed by the majority of thymocytes, by subpopulations of αβ T cells and γδ T cells and by some NK cells. Cell surface CD8α is expressed either as a disulfide-linked homodimer (CD8αα) or as a heterodimer (CD8αβ) when disulfide-bonded to a CD8 beta chain (CD8β). CD8-positive αβ T cells coexpress both CD8αα homodimers and CD8αβ heterodimers whereas some γδ T cells and NK cells express CD8αα homodimers. CD8 plays important roles in T cell activation and selection. The extracellular IgSF domain of CD8α binds to a non-polymorphic determinant on HLA class I molecules (α3 domain) and enables CD8 to function as a co-receptor with MHC class I-restricted TCR during T cell recognition of antigen. The cytoplasmic domain of CD8α associates with Lck, a Src family protein tyrosine kinase that is involved in intracellular signaling. The RPA-T8 and HIT8a monoclonal antibodies are not cross-blocking. This clone has been reported to react with a subset of peripheral blood lymphocytes, but not monocytes nor granuloytes, of baboon and both rhesus and cynomolgus macaque monkey. In general, a higher frequency of CD8+ and CD4+CD8+ lymphocytes are observed in non-human primates compared to normal human donors. Application: Flow cytometry (Routinely Tested); Source: https://www.bdbiosciences.com/en-de/products/reagents/flow-cytometry-reagents/research-reagents/single-color-antibodies-ruo/v500-mouse-anti-human-cd8.560774

SK1: CD8 is intended for in vitro diagnostic use in the identification of cells expressing CD8 antigen. Application: Flow cytometry; Source: https://www.bdbiosciences.com/en-de/products/reagents/flow-cytometry-reagents/clinical-diagnostics/single-color-antibodies-asr-ivd-ce-ivd/cd8-percp.345774

HIB19: The HIB19 monoclonal antibody specifically binds to the 95 kDa type I transmembrane CD19 glycoprotein. CD19 is expressed during all stages of B-cell maturation and differentiation, except on plasma cells. CD19 is also present on follicular dendritic cells. It is not found on T cells or on normal granulocytes. CD19 is a signal transduction molecule that regulates B cell development, activation, proliferation and differentiation. It associates with the complement receptor 2 (CD21), TAPA-1 (CD81), Leu 13, and/or MHC class II to form a signal transduction complex on the surface of B cells. Anti-CD19 clone HIB19 partially blocks the binding of clone B43, another CD19-specific monoclonal antibody. Application: Flow cytometry (Routinely Tested); Source: https://www.bdbiosciences.com/en-de/products/reagents/flow-cytometry-reagents/research-reagents/single-color-antibodies-ruo/fitc-mouse-anti-human-cd19.555412

L128: The CD27 antibody, clone L128, is derived from hybridization of mouse Sp2/0 cells with spleen cells from BALB/c mice immunized with activated peripheral blood lymphocytes. The CD27 antibody recognizes a 110–120-kilodalton (kDa) disulfide-linked homodimer comprised of two 55-kDa polypeptide chains. The CD27 antigen is a lymphocyte-specific member of the tumor necrosis factor receptor (TNFR) super family, which also includes nerve growth factor receptor, CD30, CD40, CD95 (Fas), CD120a, CD120b, CD134 (OX 40), and CD137. The CD27 antigen is also known as S152, T14, TNFRSF7, and Tp55. Application: Flow cytometry (RUO GMP); Source: https://www.bdbiosciences.com/en-de/products/reagents/flow-cytometry-reagents/clinical-discovery-research/single-color-antibodies-ruo-gmp/apc-mouse-anti-human-cd27.337169

L293: The CD28 antibody, clone L293, is derived from hybridization of Sp2/0-Ag14 mouse myeloma cells with spleen cells from BALB/c mice immunized with the HPB-ALL T-cell line. The CD28 antigen, a disulfide-linked homodimeric glycoprotein, Mr 44 kilodaltons (kd), is a cell-adhesion molecule (CAM) and functions as the ligand for CD80 (B7-1) and CD86 (B7-2) antigens, which are present on activated B lymphocytes, monocytes, and dendritic cells. Interaction of the CD28 antigen with CD80 or CD86 antigens, or both, co-stimulates CD2 and CD3 antigen/T-cell antigen receptor (TCR)–dependent T-cell–mediated proliferation and cytotoxicity. Application: Flow cytometry (RUO GMP); Source: https://www.bdbiosciences.com/en-de/products/reagents/flow-cytometry-reagents/clinical-discovery-research/single-color-antibodies-ruo-gmp/purified-mouse-anti-human-cd28.348040

HB7: CD38 is intended for in vitro diagnostic use in the identification of cells expressing CD38 antigen. Application: Flow cytometry; Source: https://www.bdbiosciences.com/en-de/products/reagents/flow-cytometry-reagents/clinical-diagnostics/single-color-antibodies-asr-ivd-ce-ivd/cd38-pe.345806

9F10: The 9F10 monoclonal antibody specifically reacts with the integrin α4 chain, that is expressed as a heterodimer with either of two β integrin subunits, β1 (CD29) or β7. The α4β1 integrin (VLA-4) is expressed on lymphocytes, monocytes, thymocytes, NK cells, and several B- and T-cell lines, and mediates binding to VCAM-1 (CD106) and the CS-1 region of fibronectin. The α4β7 integrin has a similar tissue distribution, except it is found on only a small subpopulation of thymocytes. Integrin α4β7 also binds fibronectin and VCAM-1, and has been shown in the mouse to preferentially bind the mucosal vascular addressin molecule, MAdCAM-1. This antibody is useful for studies of the expression by and function of cells that express α4 chain-containing integrins. This clone cross-reacts with a subset of peripheral blood lymphocytes, monocytes, and some granulocytes of baboon and both rhesus and cynomolgus macaque monkeys. The distribution on leukocytes is similar to that observed with human peripheral blood leukocytes. Application: Flow cytometry (Routinely Tested); Source: https://www.bdbiosciences.com/en-de/products/reagents/flow-cytometry-reagents/research-reagents/single-color-antibodies-ruo/purified-na-le-mouse-anti-human-cd49d.555501

L78: The CD69 antibody, clone L78, is derived from hybridization of mouse Sp2/0-Ag14 myeloma cells with lymph node cells from BALB/c mice immunized with a CD8+ alloantigen–directed cytotoxic T-lymphocyte (CTL) cell line. The CD69 antibody recognizes a very early human activation antigen that is a disulfide-bonded homodimer consisting of Mr 60-kilodalton (kDa) polypeptides with one or two N-linked oligosaccharides. Application: Flow cytometry (RUO GMP); Source: https://www.bdbiosciences.com/en-de/products/reagents/flow-cytometry-reagents/clinical-discovery-research/single-color-antibodies-ruo-gmp/pe-cy-7-mouse-anti-human-cd69.335792

4S.B3: The 4S.B3 monoclonal antibody specifically binds to interferon-γ (IFN-γ). The immunogen used to generate this hybridoma was partially purified human IFN-γ obtained from supernatants of human PBMC stimulated with Staphylococcus aureus. Interferon-γ (IFN-γ) is a potent multifunctional cytokine that is produced by several activated cell types including NK, NKT, CD4+TCRαβ+, CD8+TCRαβ+, and TCRγδ+ T cells. IFN-γ exerts its biological effects through specific binding to the high-affinity IFN-γ Receptor Complex comprised of IFN-γRα (CD119) and IFN-γRβ subunits. In addition to its antiviral effects, IFN-γ upregulates a number of lymphoid cell functions including the antimicrobial and antitumor responses of macrophages, NK cells, and neutrophils. In addition, IFN-γ can exert strong regulatory influences on the proliferation, differentiation, and effector responses of B cell and T cell subsets. These influences can involve IFN-γ's capacity to boost MHC class I and II expression by antigen-presenting cells as well as to direct effects on B cells and T cells themselves. Human IFN-γ is a 14-18 kDa glycoprotein containing 143 amino acid residues. Clone 4S.B3 also cross-reacts with a cytoplasmic component of peripheral blood CD3+ lymphocytes of baboon, and both rhesus and cynomolgus macaque monkeys following five-hour treatment with phorbol myristic acetate (PMA) and Ca++ ionophore (A23187) in the presence of monensin. The staining pattern of 4S.B3 in CD3+ cells is similar to that observed with peripheral blood T lymphocytes from normal human donors.

This reagent is useful for intracellular immunofluorescent staining for flow cytometric analysis to identify and enumerate IFN-γ + cells within a mixed cell population. Application: Intracellular staining (flow cytometry, Routinely Tested); Source: https://www.bdbiosciences.com/en-de/products/reagents/flow-cytometry-reagents/research-reagents/single-color-antibodies-ruo/fitc-mouse-anti-human-ifn.554551

IA6-2: The IA6-2 monoclonal antibody specifically binds to the heavy chain of human Immunoglobulin D (IgD). IgD is a member of the immunoglobulin superfamily that exists in type 1-membrane (mIgD) and soluble glycoprotein forms. mIgD is expressed on mature naïve B cells (along with membrane IgM) and serves as a B-cell receptor for antigen (BCR). In response to antigen binding, the mIgD BCR, in association with other signaling molecules including CD79a and CD79b, can transduce activating or tolerizing signals intracellularly into B lymphocytes. Application: Flow cytometry (Routinely Tested); Source: https://www.bdbiosciences.com/en-de/products/reagents/flow-cytometry-reagents/research-reagents/single-color-antibodies-ruo/pe-cy-7-mouse-anti-human-igd.561314

MQ1-17H12: The MQ1-17H12 monoclonal antibody specifically binds to the multifunctional cytokine, human Interleukin-2 (IL-2). IL-2 is produced by activated T cells and has multiple functions that can affect the growth, proliferation, differentiation and survival of many different target cell types including T cells, B cells, NK cells, monocytes and macrophages. The immunogen used to generate the MQ1-17H12 hybridoma was purified recombinant human IL-2 protein. The MQ1-17H12 antibody reportedly neutralizes the biological activity of human IL-2. Application: Intracellular staining (flow cytometry, Routinely Tested); Source: https://www.bdbiosciences.com/en-de/products/reagents/flow-cytometry-reagents/research-reagents/single-color-antibodies-ruo/pe-rat-anti-human-il-2.559334

MAb11: The MAb11 monoclonal antibody specifically binds to human tumor necrosis factor (TNF, also known as TNF-α) protein. TNF is an efficient juxtacrine, paracrine and endocrine mediator of inflammatory and immune functions. It regulates the growth and differentiation of a variety of cell types. TNF is cytotoxic for transformed cells when in conjunction with IFN-γ. It is secreted by activated monocytes/macrophages and other cells such as B cells, T cells and fibroblasts. The immunogen used to generate the MAb11 hybridoma was recombinant human TNF. The MAb11 antibody has been reported to crossreact with Rhesus Macaque TNF. Application: Intracellular staining (flow cytometry, Routinely Tested); Source: https://www.bdbiosciences.com/en-de/products/reagents/flow-cytometry-reagents/research-reagents/single-color-antibodies-ruo/v450-mouse-anti-human-tnf.561311

Human research participants

Policy information about studies involving human research participants

Population characteristics	Immunocompetent individuals with no known history of SARS-CoV-2 infection were included in the study. Individuals were enrolled after having received a primary vaccination with the ChAdOx1 nCoV-19 or one of the mRNA-vaccines (BNT162b2 or mRNA-1273) and before receiving the secondary vaccine. Three groups were included comprising homologous regimens comprising either ChAdOx1 nCoV-19 (n=55, 48.6±11.9 years of age, 35 females, 20 males) or one of the mRNA-vaccines (BNT162b2 or mRNA-1273) (n=62, 44.7±14.3 years of age, 44 females, 18 males), or a heterologous vaccine regimen comprising a ChAdOx1 nCoV-19 priming dose followed by secondary vaccination with an mRNA vaccine (n=96, 40.8±11.1 years of age, 70 females, 26 males). Three individuals (2 males with BNT162b2/BNT162b2 and mRNA-1273/mRNA-1273, respectively, and 1 female with ChAdOx1 nCoV-19/BNT162b2) were excluded from final analysis due to positive IgG towards NCAP.
Recruitment	Prospective recruitment; matching for time (14 days) after second vaccine dose with an interval of 13-18 days tolerated. All individuals were enrolled prior to the second vaccine as convenience sampling, and assignment to the vaccine groups were not randomized but determined by current guidelines. This may cause a bias in age, which was further addressed by subgroup analyses. Part of the individuals were prospectively recruited as part of this study with the same technical approach and recruitment strategy (see supplementary information).
Ethics oversight	Ethikkommission der Ärztekammer des Saarlandes

Note that full information on the approval of the study protocol must also be provided in the manuscript.

Flow Cytometry

Plots

Confirm that:

☒ The axis labels state the marker and fluorochrome used (e.g. CD4-FITC).

☒ The axis scales are clearly visible. Include numbers along axes only for bottom left plot of group (a 'group' is an analysis of identical markers).

☒ All plots are contour plots with outliers or pseudocolor plots.

☒ A numerical value for number of cells or percentage (with statistics) is provided.

Methodology

Sample preparation	Whole blood analysis
Instrument	BD FACS Canto II, BD FACSLyric
Software	BD FACSdiva software 6.1.3 BD FACSuite software v1.4.0.7047 FlowJo software 10.6.2 GraphPad Prism software 9.0 R software version 4.0.2

Cell population abundance	All blood samples were tested without further processing (i.e. no purification or cell sorting)

Gating strategy	Gating strategies are outlined in dedicated figure.

Gating of antigen-reactive T cells:
Lymphocytes were identified among total events by backgating of CD4 and/or CD8 positive cells combined with signals for size (FSC) and granularity (SSC). Hight and area signals of FSC were used to exclude doublets. CD4 T-cells were identified among single cells by CD4 positive and CD8 negative signals. Likewise, CD8 T-cells were defined as T-cells being CD8 positive and CD4 negative. Antigen-reactive cells were identified as CD4 or CD8 T-cells co-expressing the activation marker CD69 and the cytokines IFNγ, IL-2 and/or TNFα. Boundaries between "cytokine-negative" and "cytokine-positive" was defined using negative control stimulations.
For additional analysis of cytokine expression profiles, NOT Boolean Gating was used to identify all CD4 T-cells that were not CD69+IFNγ+. Among these cells CD69+IL-2+ and CD69+TNFα+ CD4 T-cells were gated and combined using OR Boolean Gating. CD69+IL-2+ and/or CD69+TNFα+ CD4 T-cells were divided into IL-2 single, TNFα single or IL-2+TNFα+ cells.
Gating of T cells and plasmablasts:
Lymphocytes were identified among total events by signals for size (FSC) and granularity (SSC). Hight and area signals of FSC were used to exclude doublets. CD3 positive T-cells were identified among single lymphocytes and further subclassified in CD4 and CD8 T-cells. Among single lymphocytes, B cells were identified by CD19 expression and subclassified in naïve, non-switched memory and switched memory B cells according to expression of IgD and CD27. Plasmablasts were identified by high expression of CD38 among switched memory B cells.

☒ Tick this box to confirm that a figure exemplifying the gating strategy is provided in the Supplementary Information.